

Studies on the Failure of the First Born Approximation in Electron Diffraction

IV. Molybdenum- and Tungsten Hexafluoride*

HANS M. SEIP and RAGNHILD SEIP

Department of Chemistry, University of Oslo, Blindern, Oslo 3, Norway

Molybdenum- and tungsten hexafluoride have been studied by electron diffraction. Three sets of complex scattering amplitudes [$f(s) = |f(s)| \cdot \exp(i\eta(s))$] have been applied. Experimentally we obtained $(\eta_W - \eta_F) = \pi/2$ at $s = 12.6 \text{ \AA}^{-1}$ and $(\eta_{Mo} - \eta_F) = \pi/2$ at $s = 22.2 \text{ \AA}^{-1}$. The corresponding theoretical values are 12.43, 13.0, 13.09 \AA^{-1} and 23.52, 24.5, 24.20 \AA^{-1} .

Thus, while the agreement is satisfactory for WF_6 , there seems to be a significant difference between the experimental and theoretical values for MoF_6 . There is no evidence for deviation from O_h symmetry in these compounds. The bond lengths with estimated standard deviations are: 1.832 (0.003) \AA (WF_6) and 1.820 (0.003) \AA (MoF_6). The corresponding root-mean-square amplitudes of vibration are 0.038 (0.003) \AA and 0.035 (0.004) \AA . The result obtained for WF_6 is in good agreement with the u value found from spectroscopic data, while the result for MoF_6 is somewhat lower than the spectroscopic value.

Three compounds have already been studied in this series of investigations, *i.e.* UF_6 ,¹ OsO_4 ,² and TeF_6 .³ The present investigations have been carried out in a way similar to those already performed. The modified molecular intensity is expressed by¹⁻³

$$I(s) = \text{const} \sum_{i \neq j} \alpha_{ij} g_{ijkl}(s) \exp(-\frac{1}{2}u_{ij}^2 s^2) \frac{\sin [(r_{ij} - \alpha_{ij} s^2)s]}{r_{ij}} \quad (1)$$

where

$$g_{ijkl}(s) = \frac{|f_i(s)| \cdot |f_j(s)|}{|f_k(s)| \cdot |f_l(s)|} \cos (\eta_i(s) - \eta_j(s)) \quad (2)$$

* Part I, II, and III, Refs. 1, 2, and 3.

If the molecule has one conformation only, α should be unity for all the distances. The α parameters have been used for control in these investigations. Besides, α may be used to determine the scale of experimental g functions (see later). κ_{ij} may be called the asymmetry constant for the bond and is zero for a symmetric distance distribution. In this case we have chosen $|f_k|$ and $|f_l|$ equal to $|f_F|$. If we assume O_h symmetry and put $\alpha_{ij} = 1$ and $\kappa_{ij} = 0$ for all the distances we obtain from eqn.(1)

$$I(s) = \text{const} [6 g_{\text{MF/FF}}(s) \exp(-\frac{1}{2}u_1^2s^2) (\sin r_1s)/r_1 + 12 \exp(-\frac{1}{2}u_2^2s^2) (\sin r_2s)/r_2 + 3 \exp(-\frac{1}{2}u_3^2s^2) (\sin r_3s)/r_3] \quad (3)$$

where M is equal to Mo or W. The indices 1, 2, and 3 refer to the bond distance, the short F...F distance, and the long F...F distance, respectively.

Only two sets of complex scattering amplitudes were available when the investigations of UF_6 ,¹ OsO_4 ,² and TeF_6 ³ were carried out. However, in the present investigations three sets were applied. We will later refer to set I, set II, and set III:

Set I has been calculated at Indiana University Research Computing Center as described by Karle and Bonham.⁴ The phase shifts in the partial waves (δ_l) were calculated according to the WKB method ($l = 0-24$) and Born's phase shift formula ($l = 25-124$). Hartree-Fock potentials⁵ were applied for atoms with atomic number ≤ 36 , while Thomas-Fermi-Dirac potentials⁶ were used for heavier atoms.

Set II has been calculated by Ibers and Hoerni⁷ using the WKB approximation and Born's phase shift formula to obtain the phase shifts. Results have been obtained for many atoms using Thomas-Fermi potentials. The values for the rest of the atoms may be found by interpolation.⁸ Hartree-Fock potentials have been applied only for a few atoms, among them fluorine. To treat all the molecules we plan to include in this series of investigations in the same way, the scattering amplitudes obtained for TF potentials were tried for all atoms. However, because of the great errors in $|f|$ for the light atoms, this did not work very well. In this case we have therefore used η_F corresponding to the TF potential and $|f_F|$ corresponding to the HF potential. The values were corrected to the applied accelerating voltage.

Set III has been calculated by a program written by J. Peacher.⁹ The phase shifts in the partial waves were calculated numerically for the lowest l values. For higher l values the WKB method and Born's phase shift formula were applied. The values of l for which the different methods have been applied, are given below for the atoms in question. It will be noticed that the number of partial waves needed to obtain convergency, varies greatly.

	F	Mo	W
δ_l calculated numerically	0-4	0-7	0-10
δ_l calculated in the WKB appr.	5-61	8-115	11-118
δ_l " by Born's phase shift formula	62-92	116-174	-

The potentials applied are the same as in set I.

WF_6 and MoF_6 were studied by electron diffraction by Braune and Pinnow¹⁰ in 1937. Scattering amplitudes calculated in the first Born approximation

were applied, and because of the double peaks corresponding to the MF bonds in the radial distribution curves (*cf.* Figs. 2 and 4), it was concluded that these molecules do not have O_h symmetry. Later Schomaker *et al.*¹¹ investigated WF_6 and MoF_6 and found similar double peaks. However, spectroscopic investigations¹²⁻¹⁵ strongly indicated O_h symmetry. As mentioned in Ref. 1 this discrepancy was explained by Glauber and Schomaker.¹⁶

EXPERIMENTAL

The sample of WF_6 was obtained from L. Light & Co. Ltd., England and the sample of MoF_6 from Baker & Adamson, New York. Both compounds were purified by distillation immediately before the data were recorded. The accelerating potential was approximately 35 kV. The nozzle temperature was approximately 15°C for WF_6 and 20°C for MoF_6 . Further data are given below:

	Nozzle to plate distance (cm)	Approximate s range (\AA^{-1})	Number of usable plates
MoF_6 :	48.04	1.50–20.25	4
	19.31	7.00–46.00	5
	19.42	7.50–46.00	2
	12.20	15.00–64.00	2
	13.13	15.00–61.50	3
WF_6 :	130.14	0.50–7.50	4
	48.03	1.50–19.75	4
	19.34	7.00–42.50	4
	12.62	15.50–60.00	4

In the case of MoF_6 photographs were recorded twice for the two shortest camera distances (≈ 19 cm and ≈ 13 cm) since the quality of the plates was not very high. The plates were photometered and the intensity data corrected in the usual way.¹⁷ The data for WF_6 could not be used for s greater than 45–50 \AA^{-1} (somewhat different on the various plates) because of noise. For MoF_6 the data were used to $s = 60 \text{\AA}^{-1}$.

STRUCTURE ANALYSIS

As in the previous investigations the structure parameters were determined by least-squares refinements on the intensity data and by comparing experimental and theoretical radial distribution (RD) curves. The RD curves are obtained by Fourier transformations of the intensity functions. An artificial damping factor ($\exp(-ks^2)$, where k is a constant) is usually applied.¹⁷ The program used for the least-squares refinements has been described previously,¹ and permits calculations of the theoretical intensity according to eqn. (1) where α , r , u , and κ may be refined.

a. WF_6 . Four observed intensity curves were obtained, each from four plates (one plate from each camera distance). Since the approximate structure parameters (distances and u values) were known,^{11,18,19} least-squares calcula-

Table 1. WF_6 . Results of least-squares calculations on four observed intensity curves (columns a–d), and mean values and standard deviations (e) obtained from these results. The parameters ($r_g(1)$ and u) are in Å. The standard deviations are given in 10^{-4} Å.

	a	b	c	d	e
s range (Å^{-1})	0.5–49.25	0.5–48.25	0.5–49.0	0.5–43.50	
r_1	1.830 ₀ (4)	1.831 ₈ (4)	1.831 ₈ (5)	1.830 ₈ (4)	1.831 ₀ (8)
r_2	2.582 (46)	2.576 (52)	2.580 (58)	2.581 (55)	2.579 ₈ (26)
r_3	3.667 (147)	3.652 (158)	3.662 (157)	3.696 (134)	3.669 ₈ (189)
u_1	0.039 ₀ (6)	0.037 ₀ (6)	0.039 ₄ (7)	0.036 ₆ (7)	0.038 ₀ (14)
u_2	0.098 (39)	0.097 (43)	0.101 (48)	0.098 (46)	0.098 ₅ (17)
u_3	0.067 (121)	0.064 (131)	0.062 (130)	0.055 (115)	0.062 ₀ (51)

The constants in the weight function (see Ref. 1) were in all cases:

$$s_1 = 6.0 \text{ Å}^{-1}, s_2 = 25.0 \text{ Å}^{-1}, W_1 = 0.1, W_2 = 0.0025.$$

tions were immediately carried out. The scattering amplitudes denoted by set I were applied. Altogether seven parameters were refined, *i.e.* three distances, three u values and the scale factor. The estimates of the parameters and their standard deviations obtained by least-squares refinements are given in Table 1 (a, b, c, and d). The mean values and standard deviations calculated from these results (giving each result the same weight) are shown in column e.* The standard deviations obtained directly by the least-squares calculations are in general found to be smaller than the values calculated from four independent determinations for the most accurately determined parameters (r_1, u_1), while the opposite result is most often found for the other parameters.^{1,3} The result obtained for r_3 in this case is an exception from the general experience.

Table 2 gives the results obtained by least-squares refinements using the intensity data from the plates taken with 130.14 cm and 48.03 cm (a), 19.34 cm (b), and 12.62 cm (c) between nozzle and plate. Here we have given the mean value for each parameter and the standard deviation for the mean calculated from the four independent results. The agreement is perhaps as good as can be expected. However, we notice a slightly low value for the bond distance in column a. A similar result was obtained for TeF_6 .³ The estimate of u_1 given in column a is also higher than obtained by using the intensities from the two shorter camera distances.

The average of the four observed intensity curves, used to obtain the results in Table 1, was further used in a series of least-squares calculations. Results are given in Table 3. The values shown in column a were obtained by using the first set of scattering functions. Fig. 1 shows the corresponding experimental (A) and theoretical (B) intensity curves. Curve C shows the differences between observed and theoretical intensities. The RD curves in

* The standard deviations for the mean values are thus $\frac{1}{2}$ times the standard deviations in column e.

Table 2. WF_s . Results for r_g (1) and u obtained by least-squares refinements. We have given the mean and the standard deviation for the mean found from four calculations. The s ranges are only approximate since the limits were usually not the same for all four calculations.

	a	b	c
Approx. s range (\AA^{-1})	0.5–19.25	7.0–42.50	16.0–49.95
s_1 (\AA^{-1})	5.0	12.0	21.0
s_2 (\AA^{-1})	13.0	25.0	30.0
W_1	0.1	0.05	0.05
W_2	0.03	0.0025	0.003
r_1 (\AA)	1.824 ₀ (15)	1.831 ₁ (3)	1.831 ₀ (5)
r_2 (\AA)	2.578 ₅ (16)	2.578 ₀ (28)	2.573 ₃ (117)
r_3 (\AA)	3.663 ₃ (57)	3.660 ₃ (34)	3.657 ₅ (235)
u_1 (\AA)	0.048 ₆ (23)	0.034 ₃ (8)	0.035 ₄ (4)
u_2 (\AA)	0.105 ₅ (3)	0.092 ₃ (13)	0.093 ₃ (57)
u_3 (\AA)	0.054 ₅ (71)	0.054 ₃ (46)	0.055 ₀ (85)

a. Results obtained by combining the data from the plates taken with the camera distances 130.14 cm and 48.03 cm.

b. Results from the plates taken with the camera distance 19.34 cm.

c. Results from the plates taken with the camera distance 12.62 cm.

Fig. 2 correspond to the intensity curves in Fig. 1. The theoretical curve (B) was obtained by a Fourier transformation using theoretical intensity data in the s range 0–50 \AA^{-1} . An envelope has been subtracted from the experimental curve (A) to compensate for the lack of data below $s = 0.75 \text{\AA}^{-1}$. A small artificial damping constant ($k = 0.0009 \text{\AA}^2$) was applied. The double peak with a minimum near 1.83 \AA corresponds to the W–F distance while the two outer peaks correspond to the F...F distances. Some values for the difference between the positions of the maxima of the double peak (Δr) are given below:

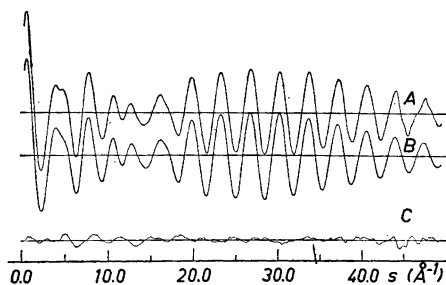


Fig. 1. WF_s . Experimental (A) and theoretical (B) intensity curves. The theoretical curve was obtained by using the results in Table 3a and the first set of scattering amplitudes. Curve C shows the difference between the curves A and B.

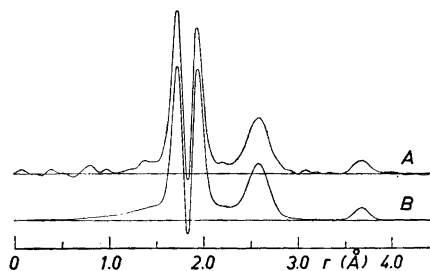


Fig. 2. WF_s . Experimental (A) and theoretical (B) RD curves calculated from the intensity curves shown in Fig. 1 with an artificial damping constant $k = 0.0009 \text{\AA}^2$.

	Δr (Å)
Experimental:	0.2104
Theoretical (first set of scattering amplitudes):	0.2137
Theoretical (second set of scattering amplitudes):	0.2086
Theoretical (third set of scattering amplitudes):	0.2032

The results in Table 3 will be discussed later (item c below).

b. MoF₆. In the case of MoF₆ we have used an average intensity curve ranging from $s = 1.50 \text{ \AA}^{-1}$ to 60.0 \AA^{-1} in all the refinements. Approximate distances and u values were also in this case known from previous investigations,^{11,18,19} and least-squares calculations could be carried out immediately. The values shown in Table 4a were obtained by using the first set of scattering amplitudes. Fig. 3 shows the corresponding experimental (A) and theoretical (B) intensity curves. Curve C gives the difference between the curves A and B. The experimental (A) and theoretical (B) RD curves shown in Fig. 4 were calculated from the intensity curves in Fig. 3 essentially as described for WF₆ ($k = 0.0009 \text{ \AA}^2$). The main difference between the RD curves in Fig. 2 and Fig. 4 is the magnitude of the split of the double peak. In this case we obtain from the RD curves ($k = 0.0009 \text{ \AA}^2$):

	Δr
Experimental:	0.125 Å
Theoretical (first set of scattering amplitudes):	0.112 Å
Theoretical (second set of scattering amplitudes):	0.103 Å
Theoretical (third set of scattering amplitudes):	0.106 Å

c. Discussion of the results for WF₆ and MoF₆. Results for a series of least-squares calculations are shown in the Tables 3 and 4. The three distances of the octahedral model were considered as independent parameters in all cases. The first three columns in the Tables 3 and 4 show the results obtained for WF₆ and MoF₆ by using respectively the first, second, and third set of scattering

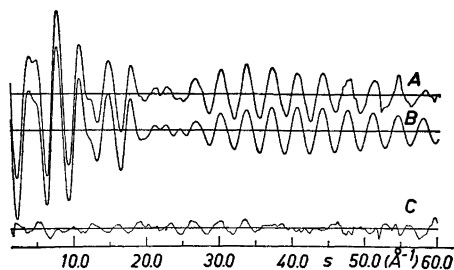


Fig. 3. MoF₆. Experimental (A) and theoretical (B) intensity curves. The theoretical curve was obtained by using the results in Table 4a and the first set of scattering amplitudes. Curve C shows the difference between the curves A and B.

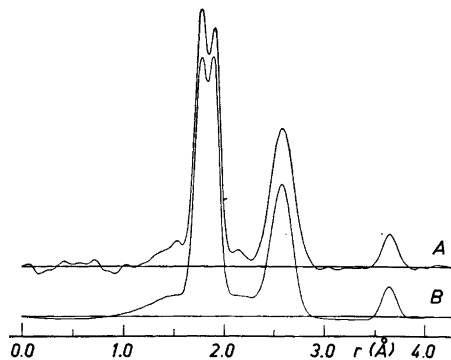


Fig. 4. MoF₆. Experimental (A) and theoretical (B) RD curves calculated from the intensity curves shown in Fig. 3 with an artificial damping constant $k = 0.0009 \text{ \AA}^2$.

Table 3. Various results (in Å) for the parameters (r_g (1) and u) in WF_6 . The standard deviations (given in parentheses) are in 10^{-4} Å.

	a	b	c	d	e
r_1	1.831 ₀ (3)	1.830 ₀ (3)	1.831 ₀ (3)	1.829 ₄ (8)	1.831 ₁ (3)
r_2	2.579 ₉ (40)	2.580 ₀ (38)	2.580 ₁ (37)	2.580 ₀ (40)	2.580 ₄ (40)
r_3	3.669 ₇ (126)	3.667 ₀ (116)	3.668 ₅ (116)	3.669 ₇ (125)	3.670 ₁ (122)
u_1	0.038 ₁ (5)	0.036 ₁ (5)	0.036 ₈ (4)	0.038 ₁ (5)	0.037 ₉ (5)
u_2	0.098 ₂ (34)	0.096 ₄ (32)	0.099 ₆ (31)	0.098 ₂ (33)	0.106 ₀ (44)
u_3	0.066 ₃ (104)	0.063 ₄ (96)	0.066 ₉ (95)	0.066 ₃ (103)	0.071 ₁ (102)

	f	g	h
r_1	1.831 ₁ (3)	1.830 ₅	
r_2	2.576 ₄ (39)	2.582	
r_3	3.669 ₇ (114)	3.665	
u_1	0.036 ₃ (5)		0.039–0.042
u_2	0.111 ₄ (43)	0.100	0.088–0.082
u_3	0.072 ₉ (96)	0.068	0.104–0.099*
			0.052

The intensity data are in the s range 0.5–49.25 Å⁻¹ in all cases. The constants in the weight function¹ are $s_1 = 6.00$ Å⁻¹, $s_2 = 25.00$ Å⁻¹, $W_1 = 0.1$, $W_2 = 0.0025$.

a-c. $\alpha = 1.0$, $\kappa = 0.0$ for all distances. a) First set, b) second set, and c) third set of scattering amplitudes.

d. κ_1 was refined; the other conditions were as in a. Result: $\kappa_1 = -1.6 \times 10^{-6}$ (0.77×10^{-6}) Å³.

e. α_1 was refined; the other conditions as in a. Result: $\alpha_1 = 0.886$ (0.04).

f. The function $g_{WF/FF}^{\text{exp}}(s)$ was applied and scaled by refining α_1 .

g. Results obtained from experimental RD curves.

h. u values obtained from spectroscopic data.¹⁸⁻²⁰ The u_2 values marked with * were obtained using the assignment suggested in Ref. 15.

amplitudes. For both compounds the distance parameters are practically the same in these three columns. As expected, the results obtained for u_2 and u_3 do not differ appreciably either, while the estimates of u_1 show variations greater than the corresponding standard deviations. Similar results have been obtained in the previous investigations.¹⁻³

The results in Tables 3d and 4d were obtained by refining κ_1 as an additional parameter. In both cases we obtain a negative value for κ_1 . A similar result was found for TeF_6 and is discussed in detail in Ref. 3.

Tables 3e and 4e show the results obtained by refining α_1 while κ_1 was kept equal to zero. For both compounds we find α_1 less than unity and an appreciable increase in u_2 . The estimates obtained for u_2 in this way may be more realistic than the results found previously, since the refinement of α_1 may compensate for errors in the theoretical scattering amplitudes and for some experimental errors. In the previous investigations we have found α_1

Table 4. Various results (in Å) for the parameters ($r_g(1)$ and u) in MoF₆. The standard deviations (given in parentheses) are in 10^{-4} Å.

	a	b	c	d	e
r_1	1.819 ₉ (6)	1.819 ₃ (7)	1.819 ₅ (7)	1.816 ₈ (11)	1.819 ₈ (6)
r_2	2.570 ₉ (26)	2.570 ₃ (31)	2.571 ₉ (31)	2.571 ₀ (26)	2.572 ₀ (25)
r_3	3.638 ₅ (72)	3.638 ₃ (84)	3.638 ₄ (84)	3.638 ₅ (71)	3.638 ₂ (69)
u_1	0.034 ₃ (5)	0.032 ₉ (7)	0.034 ₀ (6)	0.034 ₈ (5)	0.034 ₆ (5)
u_2	0.092 ₉ (22)	0.089 ₂ (26)	0.091 ₂ (26)	0.092 ₉ (22)	0.101 ₀ (27)
u_3	0.057 ₄ (60)	0.055 ₀ (70)	0.056 ₀ (70)	0.057 ₄ (59)	0.063 ₄ (58)

	f	g	h
r_1	1.819 ₉ (6)	1.819 ₂	
r_2	2.570 ₀ (23)	2.567	
r_3	3.638 ₃ (64)	3.639	
u_1	0.034 ₈ (6)		0.040—0.045
u_2	0.101 ₁ (26)	0.100	0.087—0.079
			0.110—0.105*
u_3	0.062 ₅ (54)	0.059	0.053

When nothing else is stated below the intensity data in the s range 1.5–60.0 Å⁻¹ have been used, and the constants in the weight function¹ were $s_1 = 6.00$ Å⁻¹, $s_2 = 30.0$ Å⁻¹, $W_1 = 0.1$, and $W_2 = 0.003$.

a-c. $\alpha = 1.0$, $\kappa = 0.0$ for all distances. a) First set, b) second set, and c) third set of scattering amplitudes.

d. κ_1 was refined; all other conditions as in a. Result: $\kappa_1 = -2.2 \times 10^{-6}$ (0.72×10^{-6}) Å³.

e. α_1 was refined; all other conditions as in a. Result: $\alpha_1 = 0.853$ (0.025).

f. The function $g_{\text{MoF}_6}^{\text{exp}}(s)$ was applied and scaled by refining α_1 . s range: 1.5–45 Å⁻¹.

g. Results from experimental RD curves.

h. u values obtained from spectroscopic data.¹⁸⁻²⁰ The u_2 values marked with * were obtained using the assignment suggested in Ref. 15.

less than unity for OsO₄,² but greater than unity for UF₆¹ and TeF₆.³ Thus the deviations seem rather unsystematic.

We have also carried out least-squares calculations using the experimental g functions described in the next section. The results are given in Tables 3f and 4f. The parameter values are close to those in the previous columns: the greatest change is in u_2 for WF₆.

The parameters found from RD curves are given in the next columns (g). The results are of course close to those obtained by the least-squares refinements. Figs. 2 and 4 show that the contribution from the M—F peak is not negligible in the region of the peak corresponding to r_2 . The subtraction of this contribution introduces an uncertainty particularly in the determination of u_2 . We notice that in Table 3 (WF₆) the u_2 value in (g) is closer to the value in (a) than to the value in (e). (The latter result was obtained by introducing

α_1 as an additional parameter). However, in Table 4 the agreement is excellent between u_2 in (g) and (e).

Vibrational amplitudes have been calculated for a series of hexafluorides by K. Kimura and M. Kimura¹⁸ and by Cyvin *et al.*¹⁹ The u values found by these authors are given in Table 3 h (WF₆) and Table 4h (MoF₆). However, Weinstock and Goodman¹⁵ assert that there is an error in the assignments of the fundamental frequencies used for WF₆ and MoF₆ in these u value calculations. Brunvoll²⁰ has calculated the vibrational amplitudes applying the new assignments. The results are practically the same as before for u_1 and u_3 , but the values for u_2 changed appreciably. The u_2 results found by these new calculations are included (marked with *) in the Tables 3h and 4h.

Table 5. Final results and comparison of the non-bonded distances obtained as independent parameters to the values obtained from the bond lengths.

	a	b	c	d	e	f
W—F	1.831 ₀ (30)	0.037 ₈ (30)	1.831 ₈			
F...F	2.580 (50)	0.101 (50)	2.584	2.590 ₅	0.0012	2.589
F...F	3.670 (140)	0.065 (105)	3.671	3.663 ₆	0.0048	3.659
Mo—F	1.819 ₆ (30)	0.034 ₈ (40)	1.820 ₃			
F...F	2.571 (40)	0.098 (50)	2.575	2.574 ₃	0.0015	2.573
F...F	3.639 (90)	0.060 (70)	3.640	3.640 ₆	0.0059	3.635

- a. $r_g(1)$ distances from the Tables 3 and 4 with estimated standard deviations (in 10^{-4} Å).
- b. u values from the Tables 3 and 4 with estimated standard deviations (in 10^{-4} Å).
- c. r_g distances calculated from the values in the columns a and b ($r_g = r_g(1) + u^2/r$).
- d. F...F distances calculated from the bond lengths assuming rigid octahedral molecules.
- e. Shrinkage values calculated by Cyvin *et al.*¹⁹ These values are probably not correct since one of the fundamental frequencies has probably been assigned a wrong value. However, the corrections are very small in any case.
- f. F...F distances calculated from the bond lengths and corrected for shrinkage.

Tables 3 and 4 show electron diffraction results for u_2 in the ranges 0.096—0.111 Å (WF₆) and 0.089—0.101 Å (MoF₆). By taking the mean of the results in the columns a, e, and g, we find, respectively, $u_2 = 0.101$ Å and $u_2 = 0.098$ Å with standard deviations of perhaps 0.005 Å (see Table 5). The u_2 value given above for WF₆ shows a satisfactory agreement with the spectroscopic result if the assignment given in Ref. 15 is applied (Table 3h). Since the experimental data for WF₆ were quite good (the plates taken with approximately 130 cm between nozzle and plate should greatly increase the reliability of the data at low s values), we feel that our result strongly indicates that the assignment in Ref. 15 is the correct one for WF₆.^{*} However, the agreement is not much

* The value for u_2 given in Table 2b is rather low. This result was obtained by using only the plates taken with 19.34 cm between nozzle and plate. By refining α_1 as an additional parameter the estimate of u_2 increased to 0.099 Å by using the same data.

improved for MoF₆ by using the new assignment. Since the contribution from the F...F distances to the scattered intensity is relatively larger for MoF₆ than for WF₆, it should be possible to get a better estimate for u_2 in the former case. However, the data for MoF₆ were not as good as for WF₆ as already mentioned. We thus feel that we cannot discriminate between the two assignments in this case.

The values obtained for u_1 in these investigations are seen to be lower than the results calculated from spectroscopic data. The difference is much smaller for WF₆ than for MoF₆ probably because our experimental WF₆ intensity curve is less burdened by errors. The agreement between the u_1 values obtained by the two methods is seen to be best if the first set of scattering amplitudes (*i.e.* the results in Tables 3 and 4, columns a) is chosen for both compounds. This is somewhat surprising since the method used to calculate set III is believed to be the most accurate one. However, our discussion in the next section will provide further evidence for preferring the first set. It is therefore unexpected that the standard deviations are slightly higher in Table 3a than in 3b and c. The reason may be that we had to draw a different background in the experimental intensity curves for low s values because of the differences in the absolute values of the scattering amplitudes. The standard deviations will, of course, depend heavily on the background.

Table 5 (a and b) shows the final results. The standard deviations given here include an estimate of the systematic errors. Table 5c shows the r_g distances calculated from the results in the columns a and b. As in the previous investigations we have calculated the non-bonded distances by assuming O_h symmetry. The results, after a correction for shrinkage has been made, are given in column f. The difference between the values in the columns c and f is smaller than or equal to the corresponding standard deviations.* We may conclude that there is no evidence for deviation from O_h symmetry.

SCATTERING AMPLITUDES

Experimental values for the functions

$$g_{\text{MF/FF}}^{\text{exp}}(s) = \frac{(|f_{\text{M}}| \cdot |f_{\text{F}}|)_{\text{exp}}}{(|f_{\text{F}}|^2)_{\text{theor}}} \cos(\eta_{\text{M}} - \eta_{\text{F}})_{\text{exp}} \quad (4)$$

(M = W, Mo) were obtained as described in Refs. 2 and 3. The double peak in an experimental RD curve (damped or undamped) is Fourier transformed. The values of the resulting function are given the same sign as $g_{\text{MF/FF}}$ and plotted. The envelope of this curve is, when multiplied by $\exp[(\frac{1}{2}u_1^2 + k)s^2]$, proportional to $g_{\text{MF/FF}}^{\text{exp}}$. In the case of WF₆ the four observed intensity curves were Fourier transformed separately using a damping constant $k = 0.0005 \text{ \AA}^2$. The double peaks were again Fourier transformed giving the WF

* The standard deviations in Tables 3 and 4 should perhaps be applied instead of the values in Table 5a, since the systematic errors in the distances will at least partly cancel. The difference for the short F...F distance in WF₆ is then slightly greater than the standard deviation.

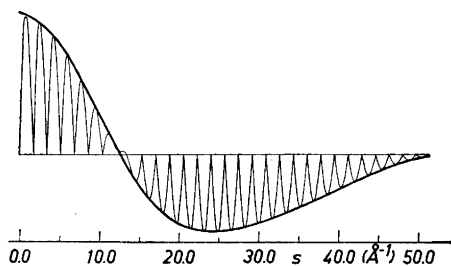


Fig. 5. WF_6 . The W-F contribution to the experimental intensity (artificially damped, $k = 0.0005 \text{ \AA}^2$) after making all values positive below $s \approx 12.5 \text{ \AA}^{-1}$ and all values negative for higher s values.

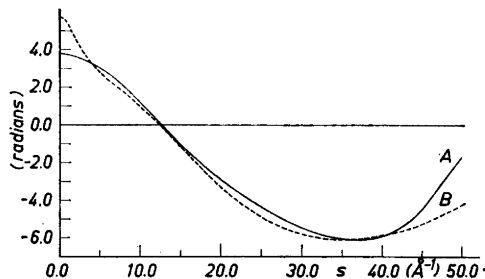


Fig. 6. WF_6 . Comparison of experimental (A) and theoretical (B) curves for $g_{WF/FF}(s)$. The first set of scattering amplitudes was applied.

contributions to the intensities (artificially damped). The signs were adjusted as described above, and the functions were plotted and the envelopes drawn. One of these curves is shown in Fig. 5. The envelopes were multiplied by $\exp[(\frac{1}{2}u_1^2 + 0.0005)s^2]$ where the u_1 values in Table 1a, b, c, and d were used. The s value corresponding to $\Delta\eta_{WF} = \pi/2$ (i.e. $g_{WF/FF}(s) = 0$) was found from each of these curves. The results were (in \AA^{-1}): 12.45, 12.49, 12.61, and 12.80, giving a mean value of 12.59 and a standard deviation of 0.16.

The average of the four experimental g functions was then calculated. It seems to be three reasonable ways to determine the scales of the experimental functions: 1) The minimum of the experimental function is chosen equal to the theoretical minimum. 2) The scale (α_1) found by the least-squares calculation using $g_{MF/FF}^{\text{exp}}(s)$ is applied. 3) The scale factor found above (method 2) is divided by the value obtained for α_1 in the least-squares calculation using the theoretical g function (cf. Tables 3e and 4e). Fig. 6 gives the averaged experimental g function scaled by method 1 (curve A). The theoret-

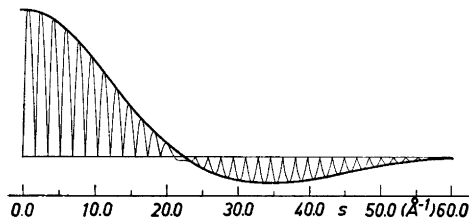


Fig. 7. MoF_6 . The Mo-F contribution to the experimental intensity (artificially damped, $k = 0.0005 \text{ \AA}^2$) plotted after making all values positive below $s \approx 22.5 \text{ \AA}^{-1}$ and all values negative for higher s values.

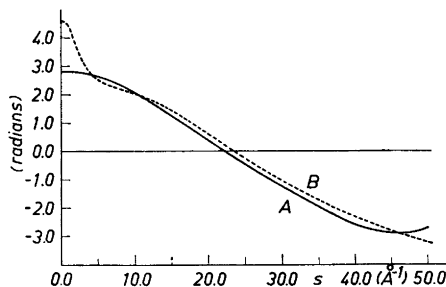


Fig. 8. MoF_6 . Comparison of experimental (A) and theoretical (B) curves for $g_{MoF/FF}(s)$. The first set of scattering amplitudes was applied.

Table 6. Experimental and theoretical s values (\AA^{-1}) corresponding to $\eta_M - \eta_F = \pi/2$.

M	a	b	c	d
W	12.6(0.20)	12.43	13.0	13.09
Mo	22.2(0.40)	23.52	24.5	24.20

a. Experimental values.

b-d. Theoretical values corresponding to b) the first set, c) the second set, and d) the third set of scattering amplitudes.

ical g function, calculated from the first set of scattering amplitudes, is shown for comparison (curve B). The scale factors found by the methods 2 and 3 are, respectively, 0.87 and 0.98 times the scale factor found by method 1.

The observed intensity curve for MoF_6 was Fourier transformed using $k = 0$, $k = 0.0005$, and $k = 0.0009$ (\AA^2). The MoF contributions were found and plotted as before (see Fig. 7). The experimental g functions have zero points at, respectively, 22.10, 22.27, and 22.38 (\AA^{-1}). The g function obtained using $k = 0.0005$ \AA^2 is shown in Fig. 8 (curve A), and the theoretical function calculated from the first set of scattering amplitudes is shown for comparison (curve B). The scale factor of the experimental function could not be determined by method 1 above, since the minimum of the theoretical curve is at $s > 60$ \AA^{-1} . Instead method 3 was used. (Method 2 gives 0.86 times the applied value (*cf.* Table 4)).

Table 6a gives the s values where $(\eta_W - \eta_F)_{\text{exp}} = \pi/2$ and $(\eta_{\text{Mo}} - \eta_F)_{\text{exp}} = \pi/2$. The columns b, c, and d give the corresponding theoretical values. The standard deviation given for WF_6 in column a is larger than the value calculated above from four determinations (theoretically we should have $\frac{1}{2} \times 0.16$) to account

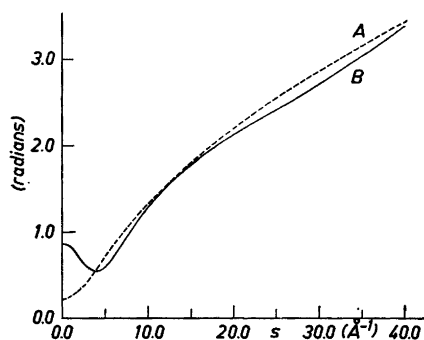


Fig. 9. Experimental (A) and theoretical (B) $\Delta\eta_{\text{WF}}(s)$ functions.

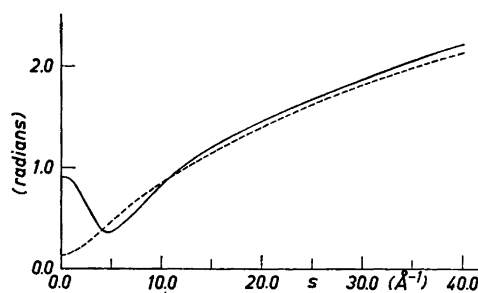


Fig. 10. Experimental (A) and theoretical (B) $\Delta\eta_{\text{MoF}}(s)$ functions.

for systematic errors. Table 6 shows that the experimental values are in best agreement with the theoretical values from set I for both compounds. The agreement is very good for WF_6 , while there seems to be a significant difference between the experimental and all the theoretical values for MoF_6 .

The experimental and theoretical values given for the split (Δr) of the double peaks (p. 2703.) are in accordance with these results. The experimental Δr value for WF_6 is between the theoretical results obtained using the first and the third set of scattering amplitudes, while the experimental split is larger than any of the theoretical ones for MoF_6 .

Figs. 9 and 10 show $\Delta\eta_{WF}$ and $\Delta\eta_{MoF}$ obtained from the experimental functions in Figs. 6 and 8 and theoretical values for $|f_M|/|f_F|$ using the first set of scattering amplitudes¹ (curves A). The theoretical $\Delta\eta$ curves (B) are shown for comparison.

Acknowledgement. The authors are grateful to Professor O. Bastiansen for many helpful discussions, Dr. A. Haaland and Cand.real. A. Almenningen for taking the diffraction photographs, and to Miss Snefrid Gullikstad for her reliable help with computer programs and other calculations.

REFERENCES

1. Seip, H. M. *Acta Chem. Scand.* **19** (1965) 1955.
2. Seip, H. M. and Stølevik, R. *Acta Chem. Scand.* **20** (1966) 385.
3. Seip, H. M. and Stølevik, R. *Acta Chem. Scand.* **20** (1966) 1535.
4. Karle, J. and Bonham, R. A. *J. Chem. Phys.* **40** (1964) 1396.
5. Strand, T. G. and Bonham, R. A. *J. Chem. Phys.* **40** (1964) 1686.
6. Bonham, R. A. and Strand, T. G. *J. Chem. Phys.* **39** (1963) 2200.
7. Ibers, J. A. and Hoerni, J. A. *Acta Cryst.* **7** (1954) 405.
8. *International Tables for X-ray Crystallography*, Kynoch Press, Birmingham 1962, Vol. III, p. 222.
9. Peacher, J. *Ph. D. Thesis*, Department of Physics, Indiana University, Bloomington, Indiana 1965.
10. Braune, H. and Pinnow, P. *Z. physik. Chem.* **B 35** (1937) 239.
11. Schomaker, V., Glauber, R., Bastiansen, O., Scheehan, W. F., Felsenfeld, G. and Ibers, J. *Chem. and Chem. Eng. Calif. Inst. Techn.* 1951–1952. 7.
12. Tanner, K. N. and Duncan, A. B. F. *J. Am. Chem. Soc.* **73** (1951) 1164.
13. Burke, T. G., Smith, D. F. and Nielsen, A. H. *J. Chem. Phys.* **20** (1954) 447.
14. Gaunt, J. *Trans. Faraday Soc.* **49** (1953) 1122.
15. Weinstock, B. and Goodman, G. L. *Advan. Chem. Phys.* **9** (1965) 169.
16. Glauber, R. and Schomaker, V. *Phys. Rev.* **89** (1953) 667.
17. Bastiansen, O. and Skancke, P. N. *Advan. Chem. Phys.* **3** (1960) 323.
18. Kimura, M. and Kimura, K. *J. Mol. Spectry.* **11** (1963) 368.
19. Meisingseth, E., Brunvoll, J. and Cyvin, S. J. *Kgl. Norske Videnskab. Selskabs, Skrifter* 1964 No. 7.
20. Brunvoll, J. *Private Communication*.

Received June 25, 1966.